CSPBankability Project Report

Draft for an
Appendix E – Thermal Energy Storage

to the
SolarPACES Guideline for
Bankable STE Yield Assessment

Document prepared by the project CSPBankability funded by the German Federal Ministry Economic Affairs and Energy under contract No. 0325293.

Gefördert durch:

Bundesministerium
für Wirtschaft
und Energie

aufgrund eines Beschlusses
des Deutschen Bundestages

Document properties

Title	CSPBankability Project Report Draft for an Appendix E – Thermal Energy Storage to the SolarPACES Guideline Bankable STE Yield Assessment
Editor	Tobias Hirsch (DLR)
Author	Markus Seitz, Michael Krüger (DLR)
Contributing authors	Heiko Schenk (DLR) Bernhard Seubert (Fraunhofer ISE) Stephan Heide (DNV-GL)
Date	January 9, 2017

Index of contents

Document properties **2**

E. Storage Modeling **4**

E.1. General overview 4
E.2. Indirect two tank molten salt storage system 5
E.2.1. Schematic overview 5
E.2.2. Heat exchanger model 6
E.2.3. Storage tank model 11
E.2.4. Auxiliary variables of storage system 16
E.2.5. Pressure loss in the HTX 16
E.2.6. Auxiliary electric consumption 17
E.2.7. Default values 18
E.3. Direct two tank molten salt storage system 20
E.3.1. Schematic overview 20
E.3.2. Storage tank model 21
E.3.3. Auxiliary variables of storage system 21
E.3.4. Auxiliary electric consumption 21
E.3.5. Default values 21
E.4. Regenerator storage system 23
E.4.1. Schematic overview 23
E.4.2. Storage model 24
E.4.3. Normalization of the equations 26
E.4.4. Implementation 27
E.5. References 29

List of abbreviations **30**

E. Storage Modeling

The main advantage of concentrated solar power (CSP) systems compared to other renewable electricity technologies is the storability of thermal energy with different kinds of thermal energy storage systems. With such a system it is possible to produce electricity after sunset if there is a demand from the grid. Within this appendix a general modelling approach is presented for the calculation of different storage systems. The section E.1 gives a general overview of the subcomponent TES and introduces some general equations. The following sections describe a specific modelling for each introduced storage technologies and are divided into several sub sections for the description of the main physical effects on the annual yield calculation.

E.1. General overview

All kinds of thermal storage concepts can be simplified to a basic energy flow scheme. Such a scheme is depicted in Figure E.1. The thermal energy storage (TES) can be charged and discharged by means of a heat transfer fluid (HTF). The HTF transfers thermal energy in both ways from the solar field (SF) to the TES and from the TES to the power block (PB). During operation and shut-down of the storage system, it is necessary to consider the electric auxillary power consumption and the thermal losses of the components of the storage system.

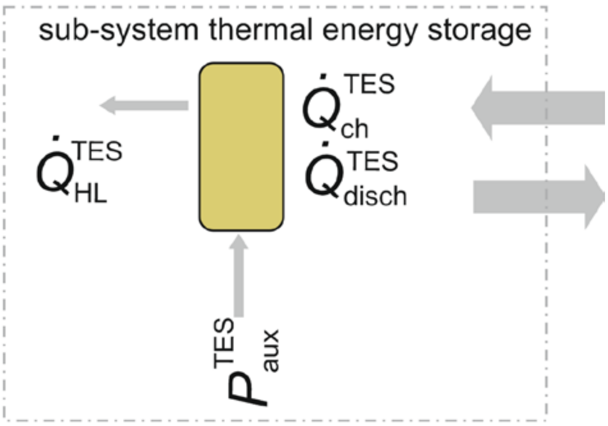

Figure E.1 Basic energy flow scheme for CSP TES systems

There are three different storage concepts described in this document:

- Indirect two tank molten salt storage
- Direct two tank molten salt storage
- Regenerator storage.

The following basic equations for the thermal power $\dot{Q}^{TES,}$ and the actual energy content $C^{TES,t}$ of the storage system apply for all types of storage systems. The thermal power $\dot{Q}^{TES}$ of the TES is calculated by the difference between the charging and discharging power of the TES. If an external heat exchanger is present, the heat loss $\dot{Q}_{\mathrm{HL,HTX}}$ must be considered.

$$\dot{Q}^{\mathrm{TES}} = \dot{Q}^{\mathrm{TES}}_{\mathrm{ch}} - \dot{Q}^{\mathrm{TES}}_{\mathrm{dis}} - \dot{Q}_{\mathrm{HL,HTX}} \tag{E.1}$$

The thermal capacity of the TES $C^{\mathrm{TES,t}}$ is calculated for every time step t by the TES capacity of the last time step $C^{\mathrm{TES,t-\Delta t}}$, the thermal power $\dot{Q}^{\mathrm{TES}}$, the anti-freeze power consumption P_{AF} and the thermal losses $\dot{Q}_{\mathrm{HL,tank}}$ of the storage tank (see Figure E.1).

$$C^{\mathrm{TES,t}} = C^{\mathrm{TES,t-\Delta t}} + \left(\dot{Q}^{\mathrm{TES}} + P_{\mathrm{AF}} - \dot{Q}_{\mathrm{HL,tank}}\right) \cdot \Delta t \tag{E.2}$$

The state of charge $f^{\mathrm{TES}}_{\mathrm{SOC}}$ describes the energy level of the TES system and is calculated by the actual energy content $\mathrm{C}^{\mathrm{TES,t}}$ divided by the rated thermal capacity $\mathrm{C}^{\mathrm{TES}}_{0}$ of the storage system. The SOC is used for a normalized evaluation of the TES.

$$f^{\mathrm{TES}}_{\mathrm{SOC}} = \frac{C^{\mathrm{TES}}}{C^{\mathrm{TES}}_{0}} \tag{E.3}$$

E.2. Indirect two tank molten salt storage system

The most common storage concept for CSP-plants with synthetic oil as heat transfer fluid (HTF) is the indirect two tank molten salt (MS) storage system. This kind of thermal energy storage (TES) is often used in commercial parabolic trough CSP-systems for the extension of electric power production after sunset and represents the state of the art for TES within the CSP area. The basic components are a cold and a hot MS tank and a heat exchanger (HTX) for the heat transfer between the MS and the HTF.

For the yield calculation of an indirect two tank MS TES a HTX model, which is described in section E.2.2 and a tank model, which is described in section E.2.3 is needed. It is also necessary to calculate auxiliary variables (section E.2.4), consider pressure losses (section E.2.5) and the auxiliary electric consumption (section E.2.6). With given default values for direct storage systems (section E.2.7), it is possible to start calculating own yield calculations with adequate approach values. At the end of section E.2 some sample calculations (section **Fehler! Verweisquelle konnte nicht gefunden werden.**) are shown to explain the calculation procedure.

E.2.1. Schematic overview

In Figure E.2 a basic scheme for the charging (left) and discharging (right) process of an indirect two tank storage is depicted. During charging, hot HTF is transferred from the solar field (SF) to the HTX of the storage system. Inside this HTX, the heat is transferred to the sensible storage material. In case of indirect two tank storage system a near eutectic mixture of sodium nitrate ($NaNO_3$) and potassium nitrate (KNO_3), so called Solar Salt[1], is used as storage material. This MS is stored on two temperature levels in cold and a hot tank. The thermal capacity can be determined by calculating the specific enthalpy difference between the hot and the cold storage tank and the usable MS mass. During the charging process, the cold MS is pumped out of its tank and heated up with the energy from the SF. The hot MS is then stored inside the hot tank. The cold HTF is then pumped to the SF. When all usable MS from the cold tank is transferred to the hot tank, the thermal storage is fully charged and the charging process has to be stopped.

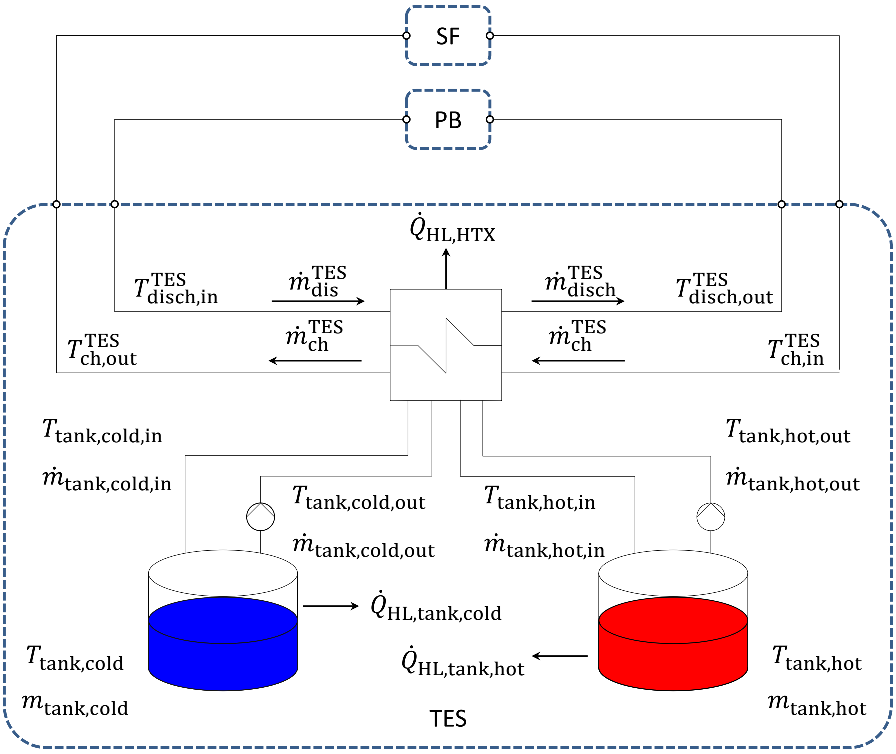

Figure E.2 Charging and discharging scheme of a two tank storage system

During discharge, the direction of flow is reversed and cold HTF from the power block PB is transferred to the HTX. Within the HTX, there is a heat transfer from the MS from the hot tank to the cold HTF. The cold MS is then stored inside the cold MS tank. The hot HTF is then transferred to the PB. When the hot tank reaches its lower usable MS level, the discharge process stops and the two tank storage is fully discharged.

E.2.2. Heat exchanger model

The heat transfer from the HTF to the MS is realized by a shell/tube HTX with baffle plates in most Spanish CSP power plants, see Figure E.3. In order to the minimization of exergy losses, the HTX is operated in a counterflow operating mode. The simplified Q-T-diagram for the rated conditions is

1

depicted in Figure E.4. Within a yield calculation it may occur that, depending on the location of the CSP-plant, the TES is charged or discharged in partial load. The reduced mass flow of the HTF and the MS through the HTX causes a reduced heat transfer between the HTF and the MS, which has to be considered during an annual yield calculation. The proposed model uses the logarithmic mean temperature difference approach (LMTD) for the consideration of the described partial load behavior of the HTX during a yield calculation. More complex or comparable models (e.g. NTU-approaches) of the HTX can be also used for the calculation of the indirect two tank storage system.

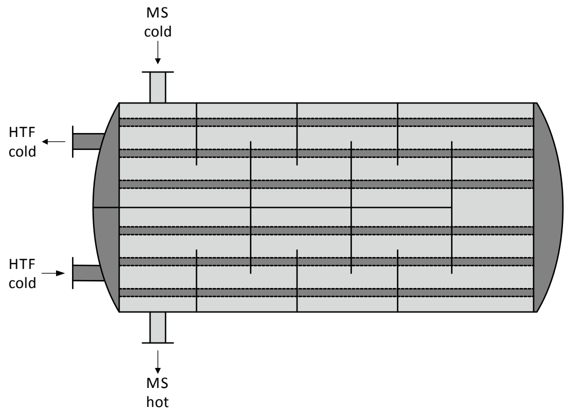

Figure E.3 Principle draft of a shell/tube HTX with counterflow layout for storage charging.

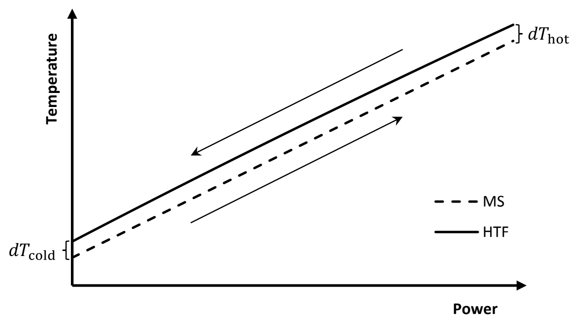

Figure E.4 Q-T-diagram for rated conditions of the HTX.

The thermal power of the HTX $\dot{Q}^{\mathrm{TES}}$ is given by a heat transfer coefficient k, the heat exchange area A and the logarithmic temperature difference ΔT_{log} of the HTX.

$$\dot{Q}^{\mathrm{TES}} = k \cdot A \cdot \Delta T_{\mathrm{log}} \quad \text{(E.4)}$$

In the following, it is presented how this general relation can be applied to the heat exchanger configuration. The aim is to describe the part load behavior as a function of nominal conditions and a part-load correction.

Heat transfer correlations at the HTX

The heat transfer coefficient of a HTX is determined by the convective heat transfer coefficient α_{HTF} inside the HTX pipes on the HTF side of the HTX and the convective heat transfer coefficient α_{MS} on the outer side of the HTX-pipes.

$$k = \frac{1}{\frac{1}{\alpha_{\mathrm{HTF}}} + \frac{1}{\alpha_{\mathrm{MS}}}} \quad \text{(E.5)}$$

The influence of the thermal conduction is very low, due to the small thickness and the high thermal conductivity of the pipe materials. For this reason, the thermal conductivity is negligible for the purpose of annual yield calculation.

The logarithmic temperature difference ΔT_{log} of the HTX is defined as

$$\Delta T_{\mathrm{log}} = \frac{\Delta T_{\mathrm{hot}} - \Delta T_{\mathrm{cold}}}{ln\left(\frac{\Delta T_{\mathrm{hot}}}{\Delta T_{\mathrm{cold}}}\right)} \quad . \tag{E.6}$$

For the calculation of the logarithmic temperature difference, the temperature difference on the hot and the cold side of the HTX, ΔT_{hot} and ΔT_{cold}, must be calculated according to

$$\Delta T_{\mathrm{hot}} = \left|T_{\mathrm{HTF,hot}} - T_{\mathrm{MS,hot}}\right| \tag{E.7}$$
$$\Delta T_{\mathrm{cold}} = \left|T_{\mathrm{HTF,cold}} - T_{\mathrm{MS,cold}}\right|. \tag{E.8}$$

For the calculation, a heat transfer coefficient kA_0 for the HTX is defined. This coefficient represents the rated conditions of the HTX and is calculated by the thermal power $\dot{Q}_0^{\mathrm{TES}}$ at rated conditions and the logarithmic temperature difference $\Delta T_{\mathrm{log,0}}$

$$kA_0 = \frac{\dot{Q}_0^{\mathrm{TES}}}{\Delta T_{\mathrm{log,0}}} \quad . \tag{E.9}$$

If the HTX is operated in part load conditions, it is necessary to calculate the part load behavior of the HTX. For this purpose, the heat transfer coefficient under rated conditions kA_0 is corrected by the factor k_{rel}, with

$$kA = kA_0 \cdot k_{\mathrm{rel}}. \tag{E.10}$$

The factor k_{rel} is calculated by ratio of the heat transfer coefficient k and the rated heat transfer coefficient k_0 . Considering equation E.5, the heat transfer coefficient k_{rel} can be written as function of the heat transfer coefficients α_{HTF} and α_{MS} and the rated heat transfer coefficients $\alpha_{\mathrm{HTF,0}}$ and $\alpha_{\mathrm{MS,0}}$.

$$k_{\mathrm{rel}} = \frac{k}{k_0} = \frac{\left(\alpha_{\mathrm{HTF,0}}\right)^{-1} + \left(\alpha_{\mathrm{MS,0}}\right)^{-1}}{\left(\alpha_{\mathrm{HTF}}\right)^{-1} + \left(\alpha_{\mathrm{MS}}\right)^{-1}} \tag{E.11}$$

For the calculation of the relative part load heat transfer coefficient α_{rel} the ratio of part load and rated mass flow is potentiated with a Nußelt-Exponent n (see Table 3 within section E.2.7). This calculation has to be performed for the HTF and the MS side of the HTX. The usage of these exponents is a common way to calculate the part load behavior of a HTX.

$$\alpha_{\mathrm{HTF,rel}} = \frac{\alpha_{\mathrm{HTF}}}{\alpha_{\mathrm{HTF,0}}} = \left(\dot{m}_{\mathrm{HTF,rel}}\right)^{n_{\mathrm{HTF}}} \tag{E.12}$$

$$\dot{m}_{\mathrm{HTF,rel}} = \frac{\dot{m}_{\mathrm{HTF}}}{\dot{m}_{\mathrm{HTF,0}}} \tag{E.13}$$

$$\alpha_{\mathrm{MS,rel}} = \frac{\alpha_{\mathrm{MS}}}{\alpha_{\mathrm{MS,0}}} = \left(\dot{m}_{\mathrm{MS,rel}}\right)^{n_{\mathrm{MS}}} \tag{E.14}$$

$$\dot{m}_{\mathrm{MS,rel}} = \frac{\dot{m}_{\mathrm{MS}}}{\dot{m}_{\mathrm{MS,0}}} \tag{E.15}$$

With equations E.12, E.15 and the mass flow correlation of the MS and the HTF mass flow

$$\dot{m}_{\mathrm{MS}} = f(\dot{m}_{\mathrm{HTF}}) \tag{E.16}$$

due to the energy balance of the HTX, the following functions for the relative heat transfer coefficients can be calculated and used for the determination of the part load heat transfer of the storage HTX. The given equation is valid for shell/tube HTX with baffle plates and is independent of the HTX rated thermal power specifications. Default values for the heat transfer coefficients for the calculation of the part load heat transfer are given in Table 4 within section E.2.7.

$$k_{\mathrm{rel}} = b_2 \cdot \left(\dot{m}_{\mathrm{HTF,rel}}\right)^2 + b_1 \cdot \dot{m}_{\mathrm{HTF,rel}} + b_0 \tag{E.17}$$

In result of equations E.4 and E.10 the transferable power of the HTX can be calculated with the following equation. It is necessary to solve the given equations in an iterative calculation (see Figure E.5).

$$\dot{Q}^{\mathrm{TES}} = kA \cdot \Delta T_{\mathrm{log}} \tag{E.18}$$

Considering heat losses of the HTX unit

For the calculation of the outlet enthalpies, it is important to distinguish between the charging and discharging mode of the HTX. The specific enthalpies of the HTF and the MS side $h_{\mathrm{ch,HTF,out}}$ and $h_{\mathrm{ch,MS,out}}$ respectively $h_{\mathrm{dis,HTF,out}}$ and $h_{\mathrm{dis,MS,out}}$ of the HTX can be calculated by the transferred heat $\dot{Q}_{\mathrm{HTX}}$, the thermal losses $\dot{Q}_{\mathrm{HL,HTX}}$ of the HTX and the HTF mass flow $\dot{m}_{\mathrm{HTF}}$.

For charging:

$$h_{\mathrm{ch,HTF,out}} = h_{\mathrm{ch,HTF,in}} - \frac{\dot{Q}^{\mathrm{TES}} + \dot{Q}_{\mathrm{HL,HTX}}}{\dot{m}_{\mathrm{ch,HTF}}} \tag{E.19}$$

$$h_{\mathrm{ch,MS,out}} = h_{\mathrm{ch,MS,in}} + \frac{\dot{Q}^{\mathrm{TES}}}{\dot{m}_{\mathrm{ch,MS}}} \tag{E.20}$$

For discharging:

$$h_{\mathrm{dis,HTF,out}} = h_{\mathrm{dis,HTF,in}} + \frac{\dot{Q}^{\mathrm{TES}}}{\dot{m}_{\mathrm{dis,HTF}}} \tag{E.21}$$

$$h_{\mathrm{dis,MS,out}} = h_{\mathrm{dis,MS,in}} - \frac{\dot{Q}^{\mathrm{TES}} + \dot{Q}_{\mathrm{HL,HTX}}}{\dot{m}_{\mathrm{dis,MS}}} \tag{E.22}$$

The heat loss $\dot{Q}_{\mathrm{HL,HTX}}$ of the HTX is determined by the heat loss coefficient $a_{\mathrm{HL,HTX}}$, the rated thermal power of the storage HTX $\dot{Q}_0^{\mathrm{TES}}$ and the temperature difference between the mean temperature of the HTX $T_{\mathrm{mean,HTX}}$ and the ambient temperature T_{amb}.

$$\dot{Q}_{\mathrm{HL,HTX}} = a_{\mathrm{HL,HTX}} \cdot \dot{Q}_0^{\mathrm{TES}} \cdot (T_{\mathrm{mean,HTX}} - T_{\mathrm{amb}}) \tag{E.23}$$

The mean temperature of the HTX is calculated as the arithmetic average of the inlet and outlet temperature of the MS. This is an appropriate approach, since the MS is on the shell side of the HTX and determines mostly the temperature of the HTX enclosure.

$$T_{\mathrm{mean,HTX}} = \frac{T_{\mathrm{MS,in}} + T_{\mathrm{MS,out}}}{2} \tag{E.24}$$

An adequate value for the heat loss coefficient $a_{\mathrm{HL,HTX}}$ for two tank storage HTX is given in Table 2 within section E.2.7.

Numerical solution of the implicit HTX equations

With this equation the physical description of the heat exchanger is complete. However, the given equations for the HTX cannot be solved analytically during a yield calculation. Figure E.5 shows a simplified flow chart for the iterative calculation of the HTX.

For the determination of the MS mass flow, a MS is estimated. This mass flow should be located within a reasonable range. At a next step the HTX is calculated with the given mass flows for the HTF and the MS side of the HTX. Therefore a guess is done for the maximum transferable power of the HTX. At a next step the logarithmic temperature difference of the HTX and the part load behavior of the HTX are calculated. After the calculation of the new HTX power, the difference of between the actual calculated power and the power of the last iteration step needs to be below numerical criteria. With this calculated result, the outlet Temperature of the MS is calculated and compared with its set point temperature. If the MS temperature deviation is below its numerical criteria, the calculation of the HTX is finished. Otherwise the next iteration with a new MS mass flow is performed, like described.

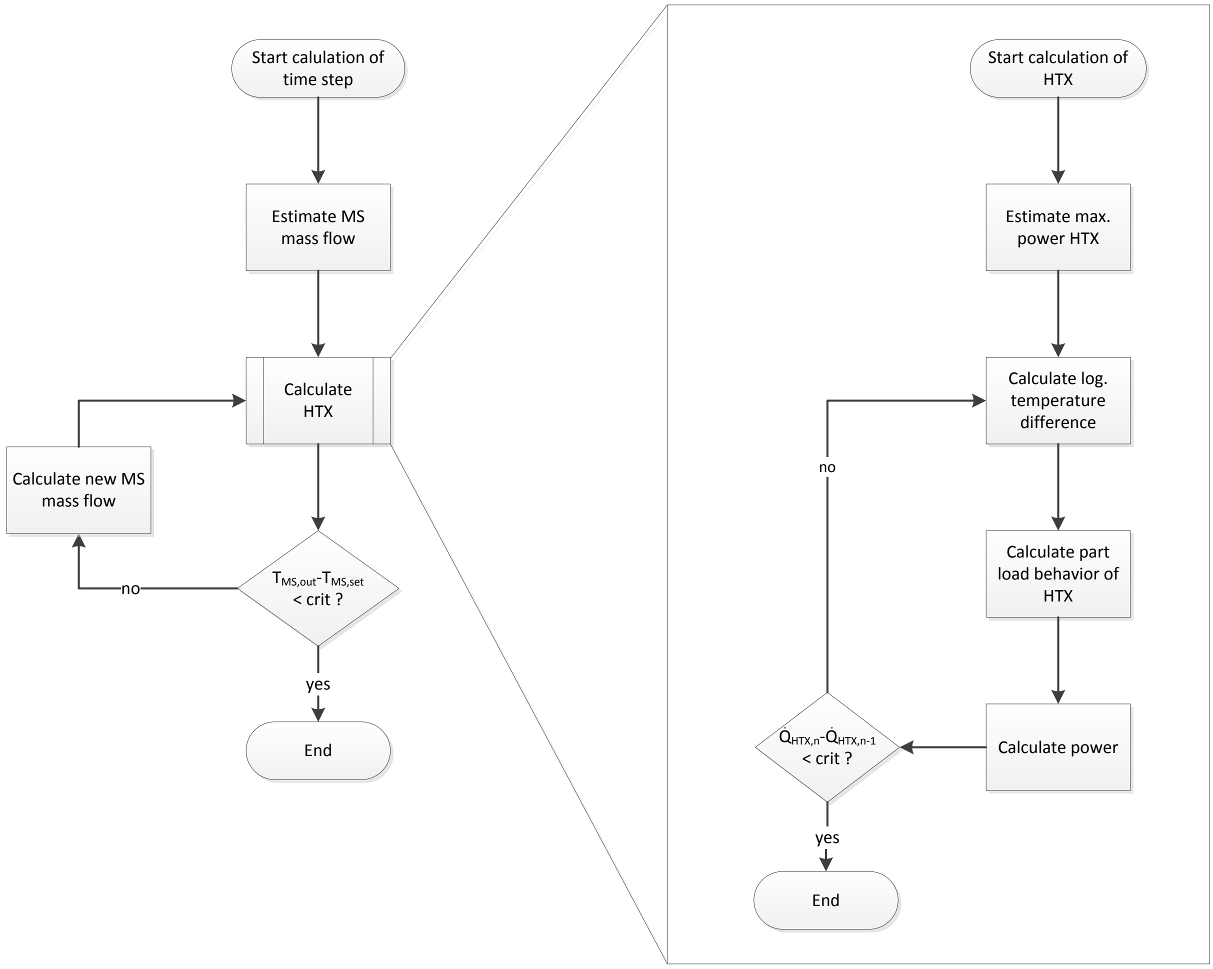

Figure E.5 Flow chart for the iterative calculation of a counterflow HTX with iterative determination of the MS mass flow.

E.2.3. Storage tank model

The MS is stored in tanks of the TES system. Depending of the state of charge of the two tank storage, the MS is kept in the hot or the cold storage tank. Each tank can store the complete MS inventory.

Each tank is described for the yield calculation by several equations:

1. Change of cold and hot tank inventory due to charging or discharging.
2. Change of cold and hot tank temperature based on an ideal mixing of the tank inventory.
3. Loss of thermal energy content by heat losses to the ambient.

Describing the charge and discharge process

The calculation for the MS mass flow of the storage tank model is based on the principle of energy conservation

$$\dot{m}_{\mathrm{ch,MS}} = \dot{m}_{\mathrm{ch,HTF}}^{\mathrm{TES}} \cdot \frac{h_{\mathrm{ch,HTF,in}} - h_{\mathrm{ch,HTF,out}}}{h_{\mathrm{ch,MS,out}} - h_{\mathrm{ch,MS,in}}} \tag{E.25}$$

for charging mode and by

$$\dot{m}_{\mathrm{dis,MS}} = \dot{m}_{\mathrm{dis,HTF}}^{\mathrm{TES}} \cdot \frac{h_{\mathrm{dis,HTF,out}} - h_{\mathrm{dis,HTF,in}}}{h_{\mathrm{dis,MS,in}} - h_{\mathrm{dis,MS,out}}} \tag{E.26}$$

for the discharging mode.

With the calculated mass flow on the MS side of the storage system for time step t, it is possible to calculate the new MS storage tank inventory distribution between hot and cold tank for the next time step.

For charging:

$$m_{\mathrm{tank,hot}}^{\mathrm{t}} = m_{\mathrm{tank,hot}}^{\mathrm{t-\Delta t}} + \dot{m}_{\mathrm{ch,MS}} \cdot \Delta t \tag{E.27}$$

For discharging:

$$m_{\mathrm{tank,cold}}^{\mathrm{t}} = m_{\mathrm{tank,hot}}^{\mathrm{t-\Delta t}} + \dot{m}_{\mathrm{dis,MS}} \cdot \Delta t \tag{E.28}$$

Mass content in the storage tanks

For the design of the storage tanks, it is important to calculate the usable MS mass $m_{\mathrm{MS,use,0}}$ of the two tank storage system. This value is defined by the rated capacity of the storage system C_0^{TES} and the rated enthalpy difference between the hot $h_{\mathrm{tank,hot,0}}$ and the cold $h_{\mathrm{tank,cold,0}}$ storage tank. The sensible and latent energy, contained in the MS below the rated cold tank temperature, is not considered within this calculation.

$$m_{\mathrm{MS,use,0}} = \frac{C_0^{\mathrm{TES}}}{h_{\mathrm{tank,hot,0}} - h_{\mathrm{tank,cold,0}}} \tag{E.29}$$

Due to the tank design it is not possible to use the entire MS mass of a storage tank. A small amount of MS $m_{\mathrm{tank,min}}$ remains in the tank sump to cover the electric heating coils and the inlet of the MS pumps. The introduced dimensionless value $L_{\mathrm{tank,min}}$ for the minimum tank level depends on the final tank layout and needs to be adjusted for an adequate calculation of the minimum tank mass. A default value for $L_{\mathrm{tank,min}}$ is given in Table 6 in section E.2.7. With the minimum tank level and the rated usable MS mass $m_{\mathrm{MS,use,0}}$, the minimum MS mass $m_{\mathrm{tank,min}}$ can be calculated.

$$m_{\mathrm{tank,min,hot}} = L_{\mathrm{tank,min}} \cdot m_{\mathrm{MS,use,0}} \tag{E.30}$$

$$m_{\mathrm{tank,min,cold}} = L_{\mathrm{tank,min}} \cdot m_{\mathrm{MS,use,0}} \tag{E.31}$$

The rated total MS mass $m_{\mathrm{MS,0}}$ inside the TES system is calculated by

$$m_{\mathrm{MS,0}} = m_{\mathrm{MS,use,0}} + m_{\mathrm{tank,min,hot}} + m_{\mathrm{tank,min,cold}}. \quad \text{(E.32)}$$

Determination of storage tank heat losses

The heat loss $\dot{Q}_{\mathrm{HL,tank}}$ of the storage tanks is calculated by the heat loss of the hot and the cold MS tank.

$$\dot{Q}_{\mathrm{HL,tank}} = \dot{Q}_{\mathrm{HL,tank,hot}} + \dot{Q}_{\mathrm{HL,tank,cold}} \quad \text{(E.33)}$$

The calculation of heat losses $\dot{Q}_{\mathrm{HL,tank,hot}}$ and $\dot{Q}_{\mathrm{HL,tank,cold}}$ based on the real geometry of storage tanks is a complex task since details on the design are often not available or the calculation based on this detailed design data is rather complex. For yield calculation it is appropriate to use a heat loss coefficient $a_{\mathrm{HL,tank}}$ that is related to the storage tank capacity. The rated storage capacity $\mathrm{C}_0^{\mathrm{TES}}$ at rated conditions is also introduced into the equations for an adequate scaling effect of the heat losses depending on the storage size.

$$\dot{Q}_{\mathrm{HL,tank,hot}} = a_{\mathrm{HL,tank,hot}} \cdot C_0^{\mathrm{TES}} \cdot \left(T_{\mathrm{tank,hot}} - T_{\mathrm{amb}}\right) \quad \text{(E.34)}$$

$$\dot{Q}_{\mathrm{HL,tank,cold}} = a_{\mathrm{HL,tank,cold}} \cdot C_0^{\mathrm{TES}} \cdot \left(T_{\mathrm{tank,cold}} - T_{\mathrm{amb}}\right) \quad \text{(E.35)}$$

The specific heat loss $a_{\mathrm{HL,tank,hot}}$ and $a_{\mathrm{HL,tank,cold}}$ link the effective heat loss of a tank to the total storage capacity $\mathrm{C}_0^{\mathrm{TES}}$ and the actual temperature difference between the tank temperature $T_{\mathrm{tank,hot,0}}$ respectively $T_{\mathrm{tank,cold,0}}$ and the ambient temperature $T_{\mathrm{amb,0}}$.

The specific heat loss value can be derived from the tank heat loss $\dot{Q}_{\mathrm{HL,tank,0}}$ at rated conditions and the corresponding rated temperatures,

$$a_{\mathrm{HL,tank,hot}} = \frac{\dot{Q}_{\mathrm{HL,tank,hot,0}}}{\mathrm{C}_0^{\mathrm{TES}} \cdot \left(T_{\mathrm{tank,hot,0}} - T_{\mathrm{amb,0}}\right)} \quad \text{(E.36)}$$

$$a_{\mathrm{HL,tank,cold}} = \frac{\dot{Q}_{\mathrm{HL,tank,cold,0}}}{\mathrm{C}_0^{\mathrm{TES}} \cdot \left(T_{\mathrm{tank,cold,0}} - T_{\mathrm{amb,0}}\right)} \quad . \quad \text{(E.37)}$$

The following paragraph illustrates a way how to determine the tank heat loss $\dot{Q}_{\mathrm{HL,tank,hot,0}}$ and $\dot{Q}_{\mathrm{HL,tank,cold,0}}$ at rated conditions. The cylindrical tank layout requires the calculation of four different partial heat losses according to Figure E.6 for the roof, the dry wall for the air/nitrogen layer, the wet wall for the MS layer and the bottom of the storage tank,

$$\dot{Q}_{\mathrm{HL,tank,0}} = \dot{Q}_{\mathrm{tank,roof}} + \dot{Q}_{\mathrm{tank,wall,dry}} + \dot{Q}_{\mathrm{tank,wall,wet}} + \dot{Q}_{\mathrm{tank,bottom}} \quad \text{(E.38)}$$

The layout assumptions for the storage tanks used in this example are given in Table 1.

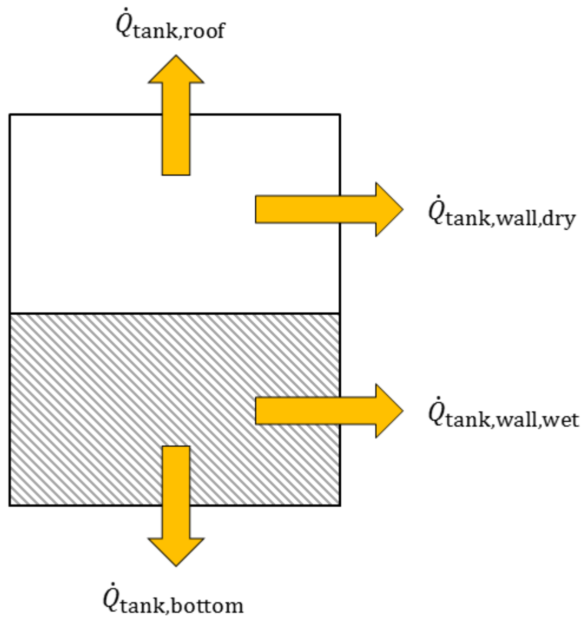

Figure E.6 Draft of a simplified cylindrical storage tank with calculated heat losses.

Table 1 Tank design assumptions for calculation of the heat losses of the storage tanks based on [Kelly 2006].

		Tank cold	Tank hot
Tank temperature	°C	292	386
Ambient temperature	°C	20	20
Roof/Wall:			
Steel	mm	6	6
Insulation	mm	300	370
Bottom:			
Steel	mm	6	6
Bricks	mm	-	60
Foam glass	mm	400	365
Isolation layer	mm	-	80
Concrete	mm	610	610

Applying elementary thermodynamic heat conduction equations, the heat loss at rated conditions can be calculated. If due to missing input data it is not possible to calculate the heat loss $a_{\mathrm{HL,tank}}$ by this approach, standard values from Table 2 within section E.2.7 can be used instead.
If there are measured or calculated heat loss values for the investigated CSP-system, which are more realistic than the proposed standard heat loss coefficient $a_{\mathrm{HL,tank}}$, it is better to use them for the yield calculation of the CSP plant.

Update of the tank temperature within a time step

With the tank heat losses, the MS mass flow and the temperature of the MS entering the tank, the calculation of the new specific enthalpy $h_{\mathrm{tank,hot}}$ and $h_{\mathrm{tank,cold}}$ of the MS tank inventory can be written as

$$h_{\mathrm{tank,hot}}^{\mathrm{t}} = \frac{m_{\mathrm{tank,hot}}^{\mathrm{t-\Delta t}} \cdot h_{\mathrm{tank,hot}}^{\mathrm{t-\Delta t}} + \left(\dot{m}_{\mathrm{tank,hot,in}} \cdot h_{\mathrm{tank,hot,in}} - \dot{Q}_{\mathrm{HL,tank,hot}}\right) \cdot \Delta t}{m_{\mathrm{tank,hot}}^{\mathrm{t}}} \quad \text{(E.39)}$$

$$h_{\mathrm{tank,cold}}^{\mathrm{t}} = \frac{m_{\mathrm{tank,cold}}^{\mathrm{t-\Delta t}} \cdot h_{\mathrm{tank,cold}}^{\mathrm{t-\Delta t}} - \left(\dot{m}_{\mathrm{tank,cold,in}} \cdot h_{\mathrm{tank,cold,in}} + \dot{Q}_{\mathrm{HL,tank,cold}}\right) \cdot \Delta t}{m_{\mathrm{tank,cold}}^{\mathrm{t}}}. \quad \text{(E.40)}$$

Please note, that a change of MS temperature in the tanks takes place in every time step (charge mode, discharge mode, or stand-still) due to heat losses. However, the discharge mass flow does not have an impact on the tank temperature since the fluid leaving the tank has the same temperature as the one within the tank. The tank temperature[2] can be determined by the calculated tank specific enthalpy by considering the material properties of MS in Appendix M. The given equations for the energy balance of the tank model cannot be solved analytically during a yield calculation. Figure E.7 shows a simplified flow chart for the iterative calculation of the tank. It is necessary to estimate a mean tank temperature for the actual time step. With this temperature it is possible to calculate the heat losses and the energy balance of the tank. As a result of the energy balance a new mean tank temperature is calculated and compared with the estimated mean temperature. If the deviation is below numerical criteria, a new outlet enthalpy is calculated for the storage tank.

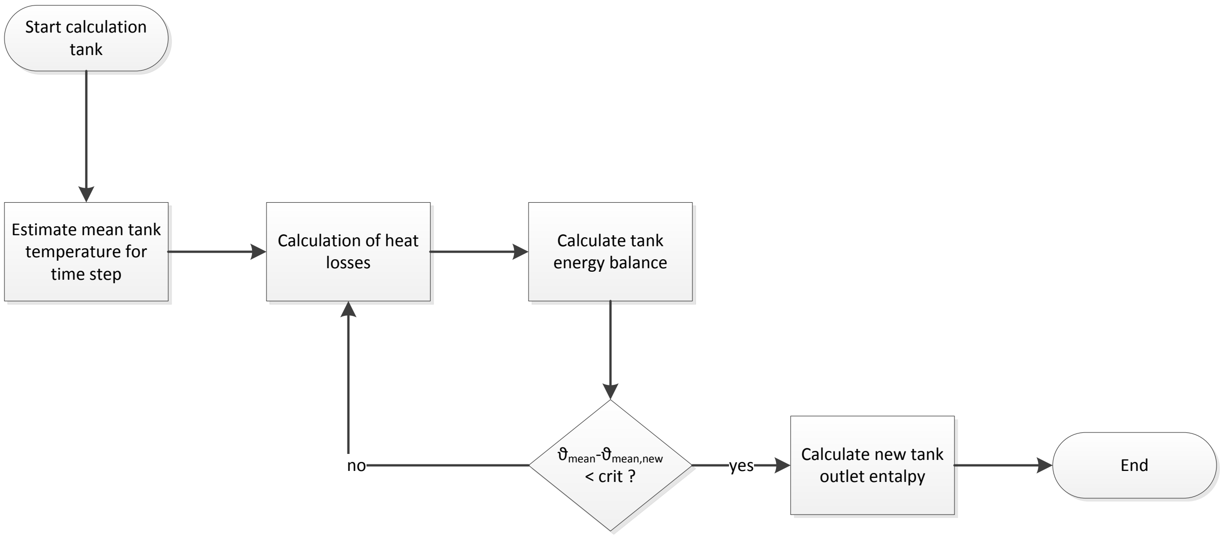

Figure E.7 Flow chart of the iterative calculation of the storage tank model.

The specific tank outlet enthalpy of the MS for the current time step should be defined as arithmetic mean value of the specific MS enthalpy at the end of the last time step and the MS enthalpy at the end of the current time step in order to be consistent with energy contents,

$$h_{\mathrm{tank,hot,out}}^{\mathrm{t}} = \frac{h_{\mathrm{tank,hot}}^{\mathrm{t}} + h_{\mathrm{tank,hot}}^{\mathrm{t-\Delta t}}}{2} \qquad \text{(E.41)}$$

$$h_{\mathrm{tank,cold,out}}^{\mathrm{t}} = \frac{h_{\mathrm{tank,cold}}^{\mathrm{t}} + h_{\mathrm{tank,cold}}^{\mathrm{t-\Delta t}}}{2} \quad . \qquad \text{(E.42)}$$

[2] The temperature of MS can be also calculated by using the specific heat capacity of MS. It must be taken into account that the specific heat capacity changes with increasing medium temperature. For that reason it would be necessary to calculate the integral sensible energy.

E.2.4. Auxiliary variables of storage system

Some auxiliary variables have to be calculated for decision process of the applied operation strategy.

Calculation of the state of charge

The state of charge $f_{\mathrm{SOC}}^{\mathrm{TES,t}}$, calculated with equation E.3 within section E.1, is an indicator for the energy content of the storage system. For the determination of the current $f_{\mathrm{SOC}}^{\mathrm{TES,t}}$, it is necessary to determine the energy content $C^{\mathrm{TES,t}}$ inside the storage tanks. The energy content of the two tank storage can be calculated with equation E.2 within section E.1.

Limitation of mass flows

For the operation strategy of the CSP-plant, it is necessary to calculate a limiting mass flow $\dot{m}_{\mathrm{lim}}^{\mathrm{TES}}$ of the two tank storage. This value is calculated at the end of the iteration process of the actual time step. Based on this mass flow, the storage mode can be determined for the next time step.

For charging:

$$\dot{m}_{\mathrm{lim,ch}}^{\mathrm{TES}} = \frac{\left(m_{\mathrm{tank,cold}} - m_{\mathrm{tank,min,cold}}\right) \cdot \left(h_{\mathrm{ch,MS,out}} - h_{\mathrm{ch,MS,in}}\right)}{\Delta t \cdot \left(h_{\mathrm{ch,HTF,in}} - h_{\mathrm{ch,HTF,out}}\right)} \tag{E.43}$$

For discharging:

$$\dot{m}_{\mathrm{dis,lim}}^{\mathrm{TES}} = \frac{\left(m_{\mathrm{tank,hot}} - m_{\mathrm{tank,min,hot}}\right) \cdot \left(h_{\mathrm{dis,MS,in}} - h_{\mathrm{dis,MS,out}}\right)}{\Delta t \cdot \left(h_{\mathrm{dis,HTF,out}} - h_{\mathrm{dis,HTF,in}}\right)} \tag{E.44}$$

E.2.5. Pressure loss in the HTX

Pressure losses in the HTF and MS part of the HTX need to be modeled appropriately in order to calculate the electric consumption of the pumps. For the thermodynamic model of the HTX there is no HTF or MS decomposition or leak flows considered. Additionally, accumulation of fluids is not possible. For that reason the mass balance for the HTF and the MS side of the HTX can be written with the following equations.

For charging:

$$\dot{m}_{\mathrm{ch,out}}^{\mathrm{TES}} = \dot{m}_{\mathrm{ch,in}}^{\mathrm{TES}} \tag{E.45}$$

$$\dot{m}_{\mathrm{ch,MS,out}} = \dot{m}_{\mathrm{ch,MS,in}} \tag{E.46}$$

For discharging:

$$\dot{m}_{\mathrm{dis,out}}^{\mathrm{TES}} = \dot{m}_{\mathrm{dis,in}}^{\mathrm{TES}} \tag{E.47}$$

$$\dot{m}_{\mathrm{dis,MS,out}} = \dot{m}_{\mathrm{dis,MS,in}} \tag{E.48}$$

The calculation of pressure losses for HTX is also based on a detailed geometry layout of the exchanger. For that reason, in early stages of modeling a nominal pressure loss is calculated for the shell and the tube side $\Delta p_{\mathrm{HTX,HTF,0}}$ and $\Delta p_{\mathrm{HTX,MS,0}}$ of the HTX.

For charging:

$$p_{\mathrm{ch,out}}^{\mathrm{TES}} = p_{\mathrm{ch,in}}^{\mathrm{TES}} - \Delta p_{\mathrm{HTX,HTF,0}} \tag{E.49}$$

$$p_{\mathrm{ch,MS,in}} = p_{\mathrm{ch,MS,out}} + \Delta p_{\mathrm{HTX,MS,0}} \tag{E.50}$$

For discharging:

$$p_{\mathrm{dis,out}}^{\mathrm{TES}} = p_{\mathrm{dis,in}}^{\mathrm{TES}} - \Delta p_{\mathrm{HTX,HTF,0}} \tag{E.51}$$

$$p_{\mathrm{dis,MS,in}} = p_{\mathrm{dis,MS,out}} + \Delta p_{\mathrm{HTX,MS,0}} \tag{E.52}$$

If the HTX is operated with reduced mass flow, the pressure drop will decrease compared to the estimated rated values $\Delta p_{\mathrm{HTX,HTF,0}}$ and $\Delta p_{\mathrm{HTX,MS,0}}$. For this reason, it is necessary to correct the rated pressure drop for the HTF and the MS side $\Delta p_{\mathrm{HTX,HTF}}$ and $\Delta p_{\mathrm{HTX,MS}}$ of the HTX with the following equations.

$$\Delta p_{\mathrm{HTX,HTF}} = \Delta p_{\mathrm{HTX,HTF,0}} \cdot \left(\frac{\dot{m}_{\mathrm{HTF}}}{\dot{m}_{\mathrm{HTF,0}}}\right)^2 \tag{E.53}$$

$$\Delta p_{\mathrm{HTX,MS}} = \Delta p_{\mathrm{HTX,MS,0}} \cdot \left(\frac{\dot{m}_{\mathrm{MS}}}{\dot{m}_{\mathrm{MS,0}}}\right)^2 \tag{E.54}$$

This approach assumes that there are constant material properties (e.g. density) for the HTF and the MS side of the HTX. General default values for $\Delta p_{\mathrm{HTX,HTF,0}}$ and $\Delta p_{\mathrm{HTX,MS,0}}$ are given in Table 6 in section E.2.7.

E.2.6. Auxiliary electric consumption

During the operation of a two tank storage, there is an auxiliary electric consumption of the TES system. The main part of auxiliary electric is needed for the MS pumps P_{pump}. A smaller percentage is needed for the power of the electric freeze protection system P_{AF} at the bottom of the storage tanks. Several minor electric consumers, for example the process control system, are not considered within the TES model.

$$P_{\mathrm{aux}}^{\mathrm{TES}} = P_{\mathrm{pump}} + P_{\mathrm{AF}} \tag{E.55}$$

$$P_{\mathrm{AF}} = P_{\mathrm{AF,hot}} + P_{\mathrm{AF,cold}} \tag{E.56}$$

The electric power of the MS pumps can be calculated by the MS mass flow $\dot{m}_{\mathrm{MS}}$, the efficiency of the MS pumps η_{pump},the density of MS ρ_{MS} and the pressure loss $\Delta p_{\mathrm{HTX,MS}}$ of the HTX. The geodetic pressure loss of such a HTX is negligible and has no crucial influence on the yield of the CSP plant.

$$P_{\text{pump}} = \frac{\dot{m}_{\text{MS}}}{\eta_{\text{pump}} \cdot \rho_{\text{MS}}} \cdot \Delta p_{\text{HTX,MS}} \tag{E.57}$$

The efficiency of the MS pump η_{pump} is determined by the isentropic efficiency $\eta_{\text{pump,isen}}$ and the electrical efficiency of the pump motor $\eta_{\text{motor,el}}$. This efficiency of the pump is due to a negligible impact on the annual yield constant during any partial load operation of the pump.

$$\eta_{\text{pump}} = \eta_{\text{pump,isen}} \cdot \eta_{\text{motor,el}} \tag{E.58}$$

The electric anti-freeze protection is only necessary if the temperature of the cold tank $T_{\text{tank,cold}}$ or the temperature of the hot tank $T_{\text{tank,hot}}$ is below the minimum temperature $T_{\text{tank,min}}$ of the used MS. When the anti-freeze heating is activated, it has to compensate all heat losses of the tank, to keep the tank inventory at the minimum MS temperature $T_{\text{tank,min}}$.

$$P_{\text{AF}} = P_{\text{AF,hot}} + P_{\text{AF,cold}} \tag{E.59}$$

$$P_{\text{AF,hot}} = \frac{a_{\text{HL,tank,hot}} \cdot Q_0^{\text{TES}}}{\eta_{\text{AF}}} \cdot \left(T_{\text{tank,min}} - T_{\text{amb}}\right) \tag{E.60}$$

$$P_{\text{AF,cold}} = \frac{a_{\text{HL,tank,cold}} \cdot Q_0^{\text{TES}}}{\eta_{\text{AF}}} \cdot \left(T_{\text{tank,min}} - T_{\text{amb}}\right) \tag{E.61}$$

In most cases the efficiency of the electric heating system is so high that it can be assumed $\eta_{\text{AF}} \approx 1$. Normally the cold tank reaches first the minimum MS temperature. For this case it is possible to use MS from the hot tank to heat up the cold MS. Only when the hot tank reaches its lower mass level, the electric anti-freeze heating prevents freezing damage within the storage system.

E.2.7. Default values

With the given default values within this section, a yield calculation can be calculated. During the project duration, more equipment is usually specified. In that case more realistic values can be used for the calculation of the annual yield of the CSP power plant. It should be also noted that default values are only valid for typical storage tank layouts with a minimum capacity of 1,000 MWh.

Table 2 Heat loss coefficients for the calculation of heat losses of an indirect 2 tank storage

Reference value	Default value	Range	Uncertainty	unit
$\boldsymbol{a}_{\mathbf{HL,HTX}}$	$9.80 \cdot 10^{-7}$	n.a.	n.a.	$\frac{1}{\mathrm{K}}$
$\boldsymbol{a}_{\mathbf{HL,tank,hot}}$	$4.07 \cdot 10^{-7}$	n.a.	n.a.	$\frac{1}{\mathrm{K\,h}}$
$\boldsymbol{a}_{\mathbf{HL,tank,cold}}$	$4.86 \cdot 10^{-7}$	n.a.	n.a.	$\frac{1}{\mathrm{K\,h}}$

In [Effenberger 2009] the Nusselt coefficient is given for the HTF and the MS side.

Table 3 Nusselt coefficients for the calculation of the heat exchanger

Reference value	Default value	Range	Uncertainty	unit
$\boldsymbol{n}_{\mathbf{HTF}}$	0.8	n.a.	n.a.	–
$\boldsymbol{n}_{\mathbf{MS}}$	0.61	n.a.	n.a.	–

Table 4 Heat transfer coefficients for the calculation of the heat exchanger of an indirect 2 tank storage

Reference value	Default value	Range	Uncertainty	unit
$\boldsymbol{b}_{\mathbf{0}}$	-0.2732	n.a.	n.a.	–
$\boldsymbol{b}_{\mathbf{1}}$	1.1830	n.a.	n.a.	$\frac{\mathrm{s}}{\mathrm{kg}}$
$\boldsymbol{b}_{\mathbf{2}}$	0.0906	n.a.	n.a.	$\frac{\mathrm{s}^2}{\mathrm{kg}^2}$

Table 5 Efficiencies of an indirect two tank storage

Reference value	Default value	Range	Uncertainty	unit
$\boldsymbol{\eta}_{\mathbf{AF}}$	1	n.a.	n.a.	–
$\boldsymbol{\eta}_{\mathbf{pump,isen}}$	0.8	n.a.	n.a.	–
$\boldsymbol{\eta}_{\mathbf{motor,el}}$	0.85	n.a.	n.a.	–

Table 6 Geometric design values of an indirect two tank storage

Reference value	Default value	Range	Uncertainty	unit
$\boldsymbol{L}_{\mathbf{min}}$	5	n.a.	n.a.	%
$\boldsymbol{\Delta p}_{\mathbf{HTX,HTF}}$	4.5	n.a.	n.a.	bar
$\boldsymbol{\Delta p}_{\mathbf{HTX,MS}}$	3.5	n.a.	n.a.	bar

E.3. Direct two tank molten salt storage system

If molten salt (MS) is used as the heat transfer fluid (HTF) within the solar field (SF), a direct thermal energy (TES) storage system can be used. This means, that there no heat exchanger is necessary for the heat exchange between the HTF and the storage medium.

For the yield calculation of a direct two tank MS TES a storage tank model is needed (see section E.3.2) that correlates the incoming and outgoing fluid streams with the change in tank level. Also heat losses affecting the temperature in the tank need to be considered in a tank model. Besides these thermodynamic variables auxiliary variables (section E.3.3) and the auxiliary electric consumption (section E.3.4) need to be considered.

E.3.1. Schematic overview

In Figure E.8 a basic scheme for the direct storage sub-system is depicted. Compared to an indirect storage with clear charging and discharging operation mode, a direct storage is charged and discharged at the same time.

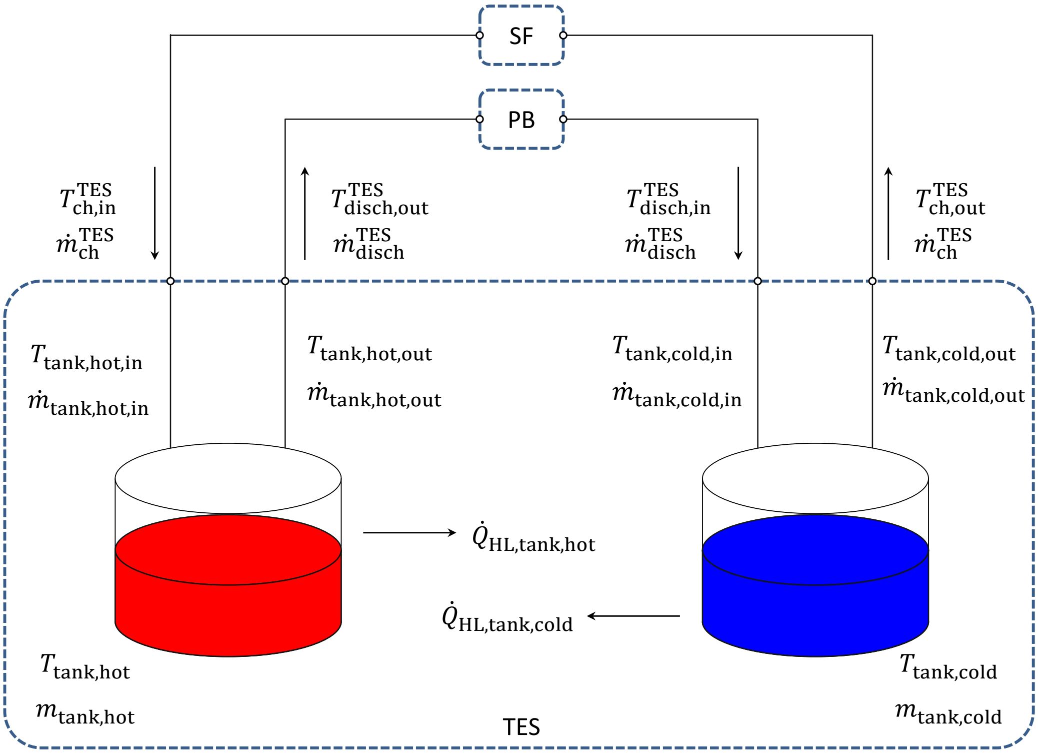

Figure E.8 Charging and discharging scheme of a two tank storage system

If the SF is in operation, cold MS is pumped from the cold tank to the parabolic trough collectors or the receiver at the top of a MS tower. The heated MS runs into the hot storage tank and is stored at a higher temperature level than in the cold tank. For electricity production, the PB is fed with MS from the hot tank storing the cooled MS in the cold tank. By this system behavior the SF and the PB are completely separated during the normal operation.

E.3.2. Storage tank model

The calculation of a direct TES is much easier than the calculation of an indirect TES within section E.2 since the impact of the heat exchanger does not need to be modeled. The calculation of the direct storage tanks is nearly the same as for the indirect TES. For that reason the equations in section E.2.3 can be used for the modeling of an indirect TES system. The only exception is the paragraph "Describing the charge and discharge process", which is not necessary for the direct TES system.

E.3.3. Auxiliary variables of storage system

Some auxiliary variables have to be calculated to be available for consideration in the applied operation strategy. The calculation of the current state of charge (SOC) is done by the general equations for the TES system given within section E.1.

Limitation of mass flows

The limiting mass flow $\dot{m}_{\mathrm{lim}}^{\mathrm{TES}}$ of the direct two tank storage is calculated by the mass of the cold MS tank. If the cold storage tank reaches its minimum fluid level, the MS mass flow which runs the PB limits the mass flow that could be heated in the SF. The maximum solar field mass flow acceptable by the storage can be determined by the discharge mass flow to the power block and the remaining mass of storage media in the cold tank,

$$\dot{m}_{\mathrm{lim}}^{\mathrm{TES}} = \frac{m_{\mathrm{tank,cold}} - m_{\mathrm{tank,min,cold}}}{\Delta t} + \dot{\mathrm{m}}_{\mathrm{hot,out}}^{\mathrm{TES}} \quad . \tag{E.62}$$

E.3.4. Auxiliary electric consumption

The calculation procedure for the auxiliary electric consumption of a direct TES system is similar to the one described in section E.2.6 for the indirect systems.

E.3.5. Default values

With the given default values within this section, a yield calculation can be calculated. During the project duration, more equipment is usually specified. In that case more realistic values can be used for the calculation of the annual yield of the CSP power plant. It should be also noted that default values are only valid for typical storage tank layouts with a minimum capacity of 1,000 MWh.

Table 7 Heat loss coefficients for the calculation of heat losses of a direct two tank storage

Reference value	Default value	Range	Uncertainty	unit
$\boldsymbol{a}_{\mathbf{HL,tank,hot}}$	$1.3 \cdot 10^{-7}$	n.a.	n.a.	$\frac{1}{\mathrm{K\,h}}$
$\boldsymbol{a}_{\mathbf{HL,tank,cold}}$	$2.0 \cdot 10^{-7}$	n.a.	n.a.	$\frac{1}{\mathrm{K\,h}}$

Table 8 Geometric design values of a direct two tank storage

Reference value	Default value	Range	Uncertainty	unit
$\boldsymbol{L}_{\mathbf{min}}$	5	n.a.	n.a.	%

E.4. Regenerator storage system

The most common storage concept for CSP-plants with air as heat transfer fluid (HTF) is the direct flow regenerator storage system. This kind of thermal energy storage (TES) is often considered in concepts for solar tower power plants with air as HTF for the extension of electric power production after sunset. The schematic overview of the system is given by section E.4.1.

For the yield calculation of a regenerator storage system, a simplified model is needed, which is described in section E.4.2 based on PhD-thesis of Dreißigacker [Dreissigacker 2014]. The normalization of the equations is described in section E.4.3. In section **Fehler! Verweisquelle konnte nicht gefunden werden.** the mathematical implementation in complex power plant simulation tools is shown.

E.4.1. Schematic overview

In Figure E.9 a basic scheme for the charging and discharging process of a regenerator storage system is depicted. During charging, hot HTF is transferred from the solar field (SF) to the TES. Inside this regenerator, the heat is transferred to the sensible storage material. In case of solar tower power plant applications, refractory or ceramic material in stacked forms or packed beds – or in case of low price options packed bed of natural stones – is used as storage material.
During discharge, the direction of flow is reversed and cold HTF from the power block (PB) is directed to the regenerator. Within the TES, there is a heat transfer from the hot inventory to the cold HTF.

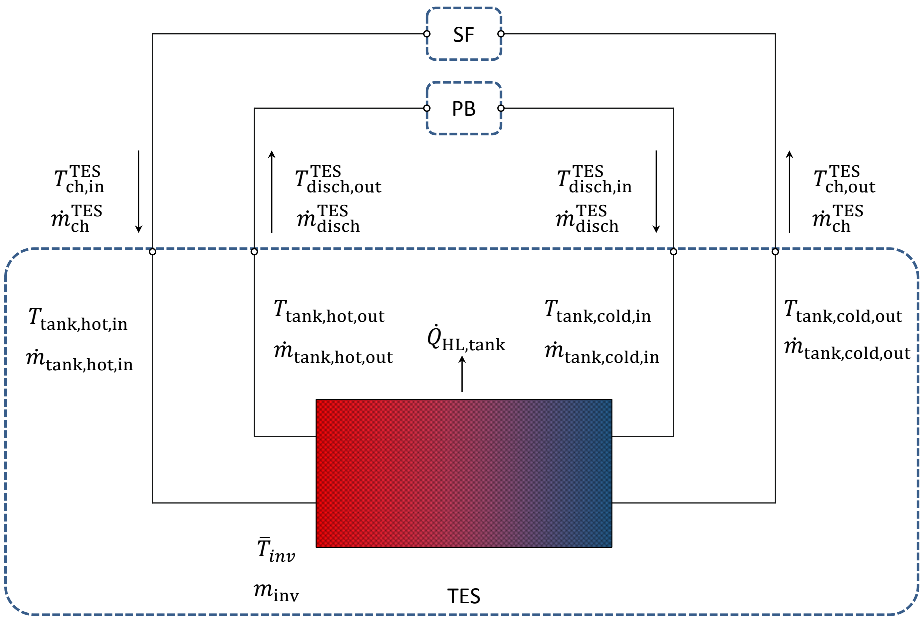

Figure E.9 Charging and discharging scheme of a regenerator storage system

E.4.2. Storage model

In contrast to two tank molten salt storage, regenerator storage is a fully dynamic component, which makes it necessary to calculate the time-related and local temperature distribution.
The partial differential equations for the description of the thermal behavior of a solid media storage are directly based on heat balances over a discrete volume. In this case, the solid is not considered to consist of a composition of individual independent bodies but as a continuous porous medium. The balancing area extends over the inlet and outlet of the storage bed. In case of packed beds, the modeling of the heat conduction via the point-shaped contacts of the individual particles in the bed takes place via effective quantities in the axial and radial direction according to [Wakao 1982]. According to [Ismail 1999], the differential equations of the heat balance in cylinder coordinates for the fluid (E.63) and solid phase (E.64) are:

$$\varepsilon\rho_F c_F\left(\frac{\partial T_F}{\partial t}+w\frac{\partial T_F}{\partial z}\right)=\lambda_{F,z,eff}\frac{\partial^2 T_F}{\partial z^2}+\lambda_{F,r,eff}\left[\frac{\partial^2 T_F}{\partial r^2}+\frac{1}{r}\frac{\partial T_F}{\partial r}\right]+\alpha_V a_V\left(T_S-T_F\right)-k_W a_W\left(T_F-T_0\right) \qquad \text{(E.63)}$$

$$\left(1-\varepsilon\right)\rho_S c_S\frac{\partial T_S}{\partial t}=\lambda_{S,z,eff}\frac{\partial^2 T_S}{\partial z^2}+\lambda_{S,r,eff}\left[\frac{\partial^2 T_S}{\partial r^2}+\frac{1}{r}\frac{\partial T_S}{\partial r}\right]+\alpha_V a_V\left(T_F-T_S\right) \qquad \text{(E.64)}$$

Where ρ is the density, c is the specific heat capacity, $\lambda_{,\mathrm{eff}}$ is the effective heat conduction in the axial (z) and radial (r) directions, α_V is the heat transfer coefficient, k_W is the overall heat transfer coefficient through the lateral surface of the storage, a_V is the specific heating surface, a_W specific lateral surface and w the fluid velocity in the bed. The void fraction ε is the fluid volume divided by the total volume of the storage.

Within this set up it is assumed that the heat conduction resistance inside of the solid is negligible and the heat transport between the fluid and the solid is determined only by the heat transfer coefficient. Depending on the thickness and the thermal conductivity of the material, however, high heat transfer resistances sometimes arise in the solid. In order to take into account this heat transfer in the storage inventory itself and to develop a compact formulation of the heat balance equations, suitable simplifications are made in the following on the differential equation (E.63) and (E.64).

In a first step, it is assumed that constant material values and adiabatic boundary conditions at the walls exist. The latter assumption leads to the fact that in the case of a uniform inflow of the bed, no thermal gradients transversal to the flow direction in the fluid occur. Based on this assumption the two-dimensional heat balance equations can be converted into a one-dimensional form. In order to take heat transfer inside the solid material into consideration, the thermal conductivity in the solid is modelled in a simplified manner via an effective heat transfer coefficient k_{eff} [VDI 2010] which comprises the heat transfer between wall and fluid and an additional impact of the heat transferred inside the storage material. This heat transfer coefficient corresponds to a time average value as a function of the charging or discharging duration, the heat transfer coefficient, the characteristic length and the material properties. Particularly in the case of storage material with high heat-conducting resistance, it is necessary to take into account the effective heat transport in the storage body in this manner. According to [VDI 2010] the adapted heat transfer coefficients are thus obtained by:

$$\frac{1}{k_{eff}} = \frac{1}{\alpha_V} + \frac{\delta}{\lambda_S}\varphi \tag{E.65}$$

Here, α_V is the heat transfer coefficient between solid and fluid which is calculated according to [VDI 2010], δ is the thickness of the storage material, λ_S is the heat conductance of the brick material, and φ is a form factor which is calculated from approximation functions of the Fourier heat conduction equation [Hausen 1950] depending on the geometry, material values, and the duration of the charging or discharging and can be found also in [VDI 2010].

Here the equations of pebble beds are exemplarily indicated. For spherical bodies with diameter *d*:

$$\frac{1}{k_{eff}} = \frac{1}{\alpha_V} + \frac{d}{2\lambda_S}\varphi \tag{E.66}$$

$$\varphi = \begin{cases} 0.1 - 0.00143\dfrac{d^2}{a_S\tau}, & \text{if } \dfrac{d^2}{a_S\tau} \le 20 \\ \dfrac{0.357}{\sqrt{3 + \dfrac{d^2}{a_S\tau}}}, & \text{if } \dfrac{d^2}{a_S\tau} > 20 \end{cases} \tag{E.67}$$

Where τ is the charging or discharging time, and *a* is the thermal diffusivity. The heat transfer coefficient α_V is calculated here for packed beds according to [Gnielinski 1982].

In order to apply the concept of effective heat transfer coefficients, the heat transfer coefficient α_V used in Equations (E.63) and (E.64) is replaced by the effective heat transfer coefficient k_{eff}. For the regenerators examined here, gaseous media are used as heat carriers and ceramic bodies are used as storage materials. Both have low thermal conductivities, so that the influence of the axial heat conduction can be neglected in the heat balance equations. In addition, due to the negligible volumetric heat capacity compared to the solid, the storage term of the fluid is not taken into account. The resulting one-dimensional heat balance is, according to [Schumann 1929]:

Fluid:

$$\varepsilon\rho_F c_F w\frac{\partial T_F}{\partial z} = k_{eff}\, a_V\left(T_S - T_F\right) \tag{E.68}$$

Solid:

$$\left(1-\varepsilon\right)\rho_S c_S \frac{\partial T_S}{\partial t} = k_{eff}\, a_V\left(T_F - T_S\right) \tag{E.69}$$

E.4.3. Normalization of the equations

As a final step for simplifying the heat balances, the space *z* is normalized by the bed length *L* and the time *t* by the charging or discharging period τ.

Spatial:

$$\partial\eta = \frac{\partial z}{L} \tag{E.70}$$

Temporal:

$$\partial\xi = \frac{\partial t}{\tau} \tag{E.71}$$

Where η is the normalized length and ξ is the normalized time.
With the assumptions and standardizations presented here, the heat balances of both phases can be converted into a compact formulation.

Fluid:

$$\frac{\partial T_{\mathrm{F}}}{\partial\eta} = \Lambda\left(T_{\mathrm{S}} - T_{\mathrm{F}}\right), \quad \text{with } \Lambda = \frac{k_{\mathrm{eff}} a_{\mathrm{V}} V_{\mathrm{tot}}}{\dot{m}_{\mathrm{F}} c_{\mathrm{F}}} \tag{E.72}$$

Solid:

$$\frac{\partial T_{S}}{\partial\xi} = \Pi\left(T_{\mathrm{F}} - T_{\mathrm{S}}\right), \quad \text{with } \Pi = \frac{k_{\mathrm{eff}} a_{\mathrm{V}} \tau}{(1-\varepsilon)\rho_{\mathrm{S}} c_{\mathrm{S}}} \tag{E.73}$$

V_{tot} means the total volume of the bed and $\dot{m}_{\mathrm{F}}$ the mass flow.
An advantage of this notation is the simple characterization of regenerators via only two dimensionless parameters, the dimensionless regenerator length Λ and the dimensionless period duration Π. Further information on this approach can be obtained e.g. by [Schmidt 1981].
To simplify the estimation of heat losses, the thermal losses across the lateral surface are taken into account in analogy to the above procedure. With the simplifications and transformations presented above, the following results for the fluid can be obtained:

$$\frac{\partial T_{\mathrm{F}}}{\partial\eta} = \Lambda\left(T_{\mathrm{S}} - T_{\mathrm{F}}\right) - \Psi\left(T_{\mathrm{F}} - T_{0}\right), \quad \text{with } \Psi = \frac{k_{\mathrm{W}} a_{\mathrm{W}} V_{\mathrm{tot}}}{\dot{m}_{\mathrm{F}} c_{\mathrm{F}}} \tag{E.74}$$

Here, Ψ is a dimensionless heat loss parameter.
By the extended heat balance, it is possible to take into account, in a simplified form, the thermal losses in the storage dimensioning. However, the one-dimensional balancing carried out here leads to an overestimation of the thermal losses since the radial heat transport is not included.

E.4.4. Implementation

The differential equations presented in section E.4.2 and E.4.3 describe the transient thermodynamical processes in a regenerator. The differential equations are implemented using appropriate numerical discretization methods. Different discretization techniques, such as finite difference method or finite element methods (FEM), are suitable for this purpose.

The numerical transformation of the thermal differential equations is performed by discretization using differential methods. In the following, this is carried out for the thermal porosity model.

The coupled differential equations (E.71) and (E.72) describe the temperatures of the fluid T_F and the solid T_S over the normalized location η and the normalized time ξ as a function of the dimensionless parameters Π and Λ.

For the implementation, the coupled differential equations are discretized spatially with respect to η and temporally with respect to ξ. In the first step, a local discretization takes place in N + 1 nodes (see Figure E.10).

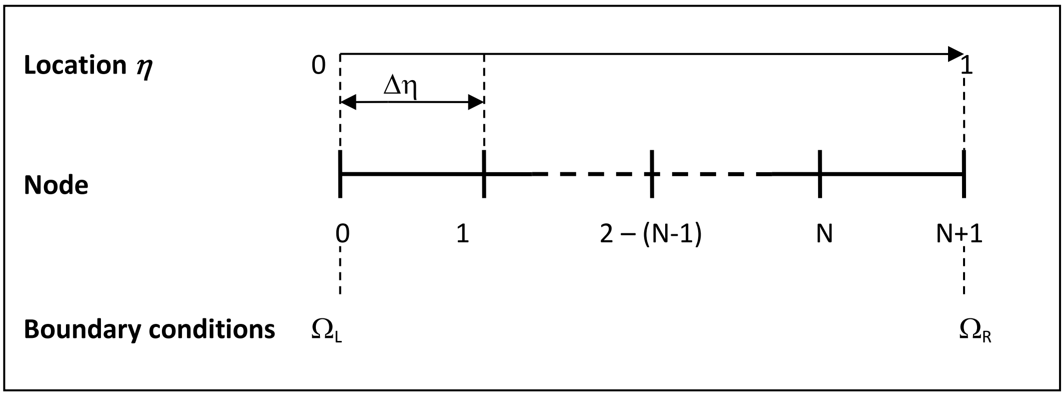

Figure E.10 : Local discretization scheme of the thermal model

The element size $\Delta\eta$ results from

$$\Delta\eta = \frac{1}{N} \tag{E.75}$$

At the outflow of the TES, adiabatic boundary conditions and at the inflow constant inlet temperatures of the fluid are specified. Due to the change of flow direction during charging and discharging, the fluid-side boundary conditions are adapted to the current operating state. A constant starting temperature is set as the starting condition during the first charging process. The temperature profile at the end of the previous state is used as the starting temperature for subsequent change from charging to discharge and vice versa. Table 9 summarizes boundary and starting conditions.

Table 9 Starting and boundary conditions of the thermal model of a regenerator storage

	Charging	Discharging
Left boundary(Ω_L)	$\left.\frac{\partial T_\mathrm{F}}{\partial \eta}\right\|_{\eta=0} = 0$	$\left.T_\mathrm{F}\right\|_{\eta=0} = T_\mathrm{F,Disch}$
Right boundary (Ω_R)	$\left.T_\mathrm{F}\right\|_{\eta=1} = T_\mathrm{F,Ch}$	$\left.\frac{\partial T_\mathrm{F}}{\partial \eta}\right\|_{\eta=1} = 0$
1st start condition	$\left.T_\mathrm{S,F}(\eta)\right\|_{\xi=0} = T_0$	
Start condition while change from discharging to charging and vice versa	$\left.T_\mathrm{S,F}(\eta)\right\|_{\xi=0,\mathrm{Disch}} = \left.T_\mathrm{S,F}(\eta)\right\|_{\xi=1,\mathrm{Ch}}$ $\left.T_\mathrm{S,F}(\eta)\right\|_{\xi=0,\mathrm{Ch}} = \left.T_\mathrm{S,F}(\eta)\right\|_{\xi=1,\mathrm{Disch}}$	

The local discretization of the solid is carried out by means of central difference quotients and that of the fluid via backward differential quotients in each case. This results in a differential-algebraic system of equations for the fluid and the solid.
The temporal discretization with respect to ξ should be carried out using a commercial simulation software (e.g. Matlab) via an internal solver e.g. according to Gear []. This is suitable for rigid differential-algebraic equation systems and is based on difference quotients with an implicit formulation of the resulting equation sets and variable increments.

E.5. References

[Effenberger 2009] Effenberger H.: Dampferzeugung, Springer-Verlag, Berlin, Germany, 1999, p. 639

[Kelly 2006] Kelly B., Kearney D.: Thermal Storage Commercial Plant Design Study for a two tank Indirect MS System, Technical Report NREL/SR-550-40166, July 2006

[Dreissigacker 2014] Dreißigacker, V.: Direkt durchströmte Feststoffwärmespeicher: Thermomechanische Untersuchungen von Schüttungen für die großtechnische Speicherung von Hochtemperaturwärme, Verlag Dr. Hut, München, Germany, 2014

[Wakao 1982] Wakao N., Kaguei S.: Heat and mass transfer in packed beds. Gordon and Braech, New York, USA, 1982

[Ismail 1999] Ismail K.A.R., Stuginsky R.: A parametric study on possible fixed bed models for pcm and sensible heat storage. Applied Thermal Engineering 19(7), pp. 757-788, 1999

[VDI 2010] Hausen, H.: N1 Heat Transfer in Regenerators. In VDI-GVC, VDI Heat Atlas. Springer-Verlag, Berlin; Heidelberg, 2010, pp. 1423-1434

[Ratzesberger 1994] Ratzesberger R., Beine B., Hahne E.: Regeneratoren mit Beton und Phasenwechselmaterial als Speichermasse. VDI-GET Tagung, Leipzig, Germany, 1994

[Hausen 1950] Hausen H: Wärmeübertragung im Gegenstrom, Gleichstrom und Kreuzstrom. Springer-Verlag, Heidelberg, Berlin, 1950

[Gnielinski 1982] Gnielinski V.: vt “Verfahrenstechnik” 16(1), p. 36/39, 1982

[Schumann 1929] Schumann T.E.W.: Heat transfer: A liquid flowing through a porous prism. J. Franklin Inst. 208(3), pp. 405-416, 1929

[Schmidt 1981] Schmidt F.W., Willmott A.J.: Thermal Energy Storage and Regeneration. McGraw-Hill Book Company, 1981

[Shampine 1999] Shampine L.F., Reichelt M.W., Kierzenka J.A.: Solving Index-1 DAEs in MATLAB and Simulink. SIAM Review 41(3), pp. 538-552, 1999

List of abbreviations

AF	Anti-freeze
CSP	Concentrated solar power
HL	Heat loss
HTF	Heat transfer fluid
HTX	Heat exchanger
MS	Molten salt
PB	Power block
SF	Solar field
SOC	State of charge
TES	Thermal energy storage